

Sorption of U(VI) onto a decarbonated calcareous soil

Yuying Zhang · Haogui Zhao · Qiaohui Fan ·
Xiaobei Zheng · Ping Li · Shengping Liu ·
Wangsuo Wu

Received: 9 November 2010 / Published online: 4 January 2011
© Akadémiai Kiadó, Budapest, Hungary 2011

Abstract Sorption of U(VI) from aqueous solution to decarbonated calcareous soil (DCS) was studied under ambient conditions using batch technique. Soil samples were characterized by XRD, FT-IR and SEM in detail and the effects of pH, solid-to-liquid ratio (m/V), temperature, contact time, fulvic acid (FA), CO₂ and carbonates on U(VI) sorption to calcareous soil were also studied in detail using batch technique. The results from experimental techniques showed that sorption of U(VI) on DCS was significantly influenced by pH values of the aqueous phase, indicating a formation of inner-sphere complexes at solid–liquid interface, and increased with increasing temperature, suggesting the sorption process was endothermic and spontaneous. Compared to Freundlich model, sorption of U(VI) to DCS was simulated better with Langmuir model. The sorption equilibrium could be quickly achieved within 5 h, and sorption results fitted pseudo-second-order model well. The presence of FA in sorption system enhanced U(VI) sorption at low pH and reduced U(VI) sorption at high pH values. In absence of FA, the sorption of U(VI) onto DCS was an irreversible process, while the presence of FA reinforced the U(VI) desorption process reversible. The presence of CO₂

decreased U(VI) sorption largely at pH >8, which might due to a weakly adsorbable formation of Ca₂UO₂(CO₃)₃ complex in aqueous phase.

Keywords Soil · U(VI) · Sorption · Desorption · FA · Carbonate

Introduction

The transport processes of radionuclides in geological materials have been widely studied for better understanding of their physicochemical behavior in natural environment [1–5]. Uranium, as one of main radionuclides in nuclear industry, is an important contaminant in the place of uranium mining and milling, and nuclear waste disposal. Under natural conditions, uranium typically exists in hexavalent form as the mobile aqueous uranyl ion (U(VI)) [6]. Its mobility in environment is determined by several complexes and coupled processes, including oxidation–reduction, precipitation–dissolution, and sorption–desorption etc. Among these processes, sorption and desorption reactions play a critical part. In the last decade, U(VI) sorption on clay minerals, oxides and natural soils has been extensively studied. XIE et al. [7] investigated U(VI) sorption onto hematite as a function of solution pH, contact time, initial concentration, temperature, calcium and magnesium ions. Influence of calcite and dissolved calcium on uranium(VI) sorption to a Hanford subsurface sediment has been examined by DONG et al. [8], and results were obtained to indicate that formation of Ca₂UO₂(CO₃)₃(aq) has suppressed uranium sorption at pH <8.4, whereas UO₂(CO₃)₃⁴⁻ has been found as the dominated speciation in solution at pH >8.4. Charge distribution (CD) model was also used to evaluate uranyl sorption on ferrihydrite, which found that a

Zhang Yuying, Zhao Haogui The same contribution to this paper.

Y. Zhang · H. Zhao · Q. Fan (✉) · X. Zheng · P. Li · S. Liu ·
W. Wu (✉)
Radiochemistry Laboratory, Lanzhou University,
Lanzhou 730000, China
e-mail: fanqiaohui@gmail.com

W. Wu
e-mail: wuws@lzu.edu.cn

W. Wu
State Key Laboratory of Applied Organic Chemistry,
Lanzhou University, Lanzhou, China

uranyl tris-carbonate surface complex, i.e. $\equiv(\text{UO}_2)(\text{CO}_3)_3^{4-}$, was formed at relatively high pH and carbonate concentration [9].

Influence of humic substances (HSs) on the sorption of radionuclides to oxides and minerals has been extensively examined in the past decades for their wide scale existence in natural soil [10–13]. Li et al. [14] found that presence of HSs enhanced Co(II) sorption on bentonite, $\gamma\text{-Al}_2\text{O}_3$ and silica at low pH and reduced the metal ion sorption at high pH values. Fan et al. [15] found that sorption isotherms of Eu(III) on HA bound MWCNTs were much higher than those of Eu(III) on bare MWCNTs, and different addition sequences of HA and Eu(III) strongly affected the sorption of Eu(III) on MWCNTs, which was ascribed to the strong complexation of HA-Eu and HA-MWCNTs. However, it was found by Ticknor et al. [16] that FA had no effect on Sr(II) sorbed to montmorillonite and also Cs(I) to quartz and U(VI) to montmorillonite, biotite, granite and quartz. In addition, in the study performed by Wang et al. [17], FA was shown to decrease Pb(II) adsorption at pH from 2 to 11.

Soil, due to its high specific surface areas, is prone to enrich toxic metal ions and thus acts as a medium for metal ions entering into the biologic food chain, causing unexpected harm to human health [18]. However, researches on general ability of soil adsorbing uranium as a function of different aqueous conditions are still scarce. In this paper, sorption of U(VI) on decarbonated calcareous soil (DCS) was investigated as a function of pH, solid-to-liquid ratio (m/V), temperature. Sorption kinetics and effects of fulvic acid (FA), carbonate and CO_2 on sorption of U(VI) to DCS were studied, and desorption tests examining effect of FA on U(VI) sorption were also performed.

Experimental

Sampling and analysis of soils

All chemicals used in the experiments were purchased as analytically pure and used without any further purification. FA was extracted from Gannan soils, using method from IHSS [19]. The original calcareous soil sample was collected from surface 0–20 cm horizon of soils in Yuzhong county of Gansu province.

The soil sample was converted to Ca-type calcareous soil (CaCS) by treating with 0.1 mol/L CaCl_2 under room temperature for 5 days, then washed with doubly distilled water until no detectable chloride was found, centrifuged at 12000 rpm, dried, and passed through a 0.2 mm sieve. Decarbonated calcareous soil (DCS) was obtained by blending former CaCS sample with HAc-NaAc (pH 4.6) buffer solution for 2 days to remove carbonate, then the

sample was washed, dried and ground to pass 0.2 mm sieve prior to use.

Selective properties of Ca-type calcareous soil (CaCS) and decarbonated calcareous soil (DCS) are presented in Table 1. Element content and mineral content of studied soils are presented in Tables 2 and 3. Data show that carbonate content decreases from 15.03% to zero when CaCS sample was transformed to DCS (Table 1). Content of CaO (Table 2) and content of calcite (Table 3) decreases from 8.73 to 1.55% and 16% to zero, respectively, therefore carbonates were basically removed from DCS.

Sorption experiments

All tests were carried out at ambient conditions. Stock suspensions of soil, NaClO_4 , uranium(VI) solution and MES (pH 6.2) buffer solution were added into polyethylene tubes to achieve desired concentrations of different components. The pH values of solutions were adjusted by adding negligible volumes of 0.1 or 0.01 mol/L HClO_4 or NaOH. The suspensions were shaken for 48 h, then centrifuged at 12000 rpm for 30 min. For CO_2 -free system, sorption tests were performed in a nitrogen atmosphere glove box.

In desorption tests, soil suspension was centrifuged (12000 rpm, 30 min) at the end of sorption experiments, then half of supernatant was pipetted out before an equal volume of background electrolyte solution with the same pH value was added. Then the mixture was shaken and centrifuged under the same conditions as in the sorption experiments.

The concentration of aqueous U(VI) was analyzed by spectrophotometry at wavelength 652 nm using U Arsenazo III complex.

XRD and FTIR analysis

DCS was characterized by Fourier transform infrared spectra (FTIR) and X-ray diffraction (XRD). The sample for the FTIR measurement was mounted on a Bruker EQUINOX55 spectrometer (Nexus) in KBr pellet at room temperature. XRD pattern of the DCS structure was obtained from a

Table 1 Selective properties of studied soils

| Sample | pH ($m/V = 1:1$) | EC ($\mu\text{S}/\text{cm}$) ($m/V = 1:2$) | CC % | SOM % |
|--------|-----------------------|---|-------|-------|
| CaCS | 8.2 | 222 | 15.03 | 1.38 |
| DCS | 7.8 | 302 | 0 | – |

EC electrical conductivity, CC carbonate content, SOM soil organic matter content, – Not determined

Table 2 Element content of studied soils

| Sample | Fe ₂ O ₃ (%) | SiO ₂ (%) | Al ₂ O ₃ (%) | MgO (%) | CaO (%) | Na ₂ O (%) | K ₂ O (%) | CO ₃ (%) |
|--------|------------------------------------|----------------------|------------------------------------|---------|---------|-----------------------|----------------------|---------------------|
| CaCS | 4.24 | 56.75 | 10.95 | 2.73 | 8.73 | 2.04 | 2.04 | 11.80 |
| DCS | 5.18 | 65.60 | 12.74 | 2.81 | 1.55 | 1.65 | 2.62 | 7.09 |

Table 3 Mineral content of studied soils

| Sample | Chlorite (%) | Mica (%) | Amphibole (%) | Quartz (%) | Feldspar (%) | Calcite (%) |
|--------|--------------|----------|---------------|------------|--------------|-------------|
| CaCS | 13 | 19 | 4 | 31 | 17 | 16 |
| DCS | 18 | 22 | 2 | 45 | 12 | 0 |

D/Max-rB equipped with a rotation anode using Cu K α radiation ($\lambda = 0.15406$ nm). The XRD device was operated at 40 kV and 80 mA. The measurements were carried out in the range of $2^\circ \leq 2\theta \leq 70^\circ$.

Results and discussion

XRD analysis

XRD patterns of CaCS sample and DCS sample are shown in Fig. 1. The XRD patterns in general show strong reflections at $2\theta = 26.6^\circ$ and $2\theta = 20.8^\circ$, both arising from quartz. The peak at $2\theta = 27.9^\circ$ is attributed to Hydromica. Small signals at $2\theta = 30.9^\circ$, 34.9° and 36.5° could be assigned to amphibole. Peaks of chlorite and feldspar are also marked in Fig. 1. Peaks arising from calcite are only found in pattern of CaCS sample, which indicates that carbonates have been removed from CaCS in the preparation of DCS.

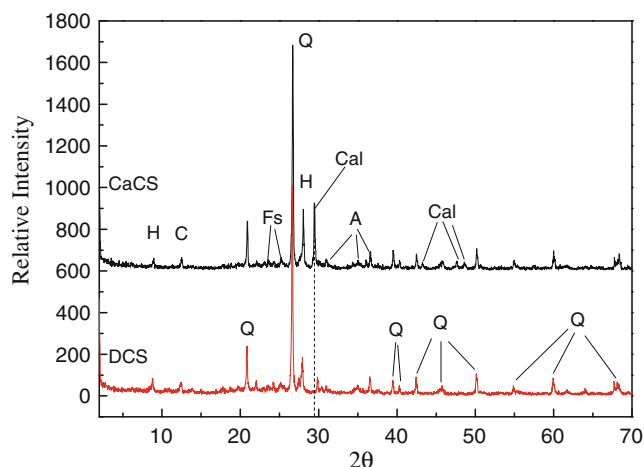


Fig. 1 XRD analysis of CaCS sample and DCS sample. H Hydromica, C Chlorite, Fs Feldspar, Q Quartz, A Amphibole, Cal Calcite

SEM measurement

SEM images of DCS sample are presented in Fig. 2a and b are showing microstructure of soil layers in different microscale magnitude, of 5000 times and 10000 times respectively. In Fig. 2a, soil particles are shown in flake or block shape. The particle size of DCS sample varies largely, from less than 10 μm to more than hundreds, and the differences in particle size are more obvious in Fig. 2b. Smaller soil particles with a higher specific surface area can contribute to a better adsorbing ability.

Kinetics of sorption process

Sorption percent of U(VI) on DCS as a function of contacted time under different m/V values is shown in Fig. 3a. It is seen that increasing sorption of U(VI) mainly occurred during the first 5 h and then reached a sorption equilibrium. According to Lu et al. [20], the fast sorption of U(VI) to DCS suggests that this process can be attributed to surface complexation and/or chemical sorption rather than physical sorption. The shaking time was fixed for 48 h for the rest of the batch experiments to make sure that equilibria were reached. In addition, sorption percent of U(VI) is obviously influenced by solid-to-liquid ratio, increasing from ~ 35 to $\sim 50\%$ at equilibrium state with m/V rising from 0.4 g/L to 0.6 g/L. In order to study the sorption kinetics of U(VI) on DCS, a pseudo-second-order rate equation was used to fit the kinetic of sorption [10, 21]:

$$\text{Sorption}\% = \frac{C_0 - C_e}{C_0} \times 100\% \quad (1)$$

$$t/C_s = 1/(K'C_{\text{max}}^2) + t/C_{\text{max}} \quad (2)$$

where C_0 (mol/L) and C_e (mol/L) represent the concentration of U(VI) in suspension and supernatant after centrifugation, respectively; K' ($\text{g mol}^{-1} \text{h}^{-1}$) is the pseudo-second-order rate constant of sorption; C_s (mol g^{-1}) is the amount of

Fig. 2 SEM images of DCS. **a** $\times 5000$, **b** $\times 10000$

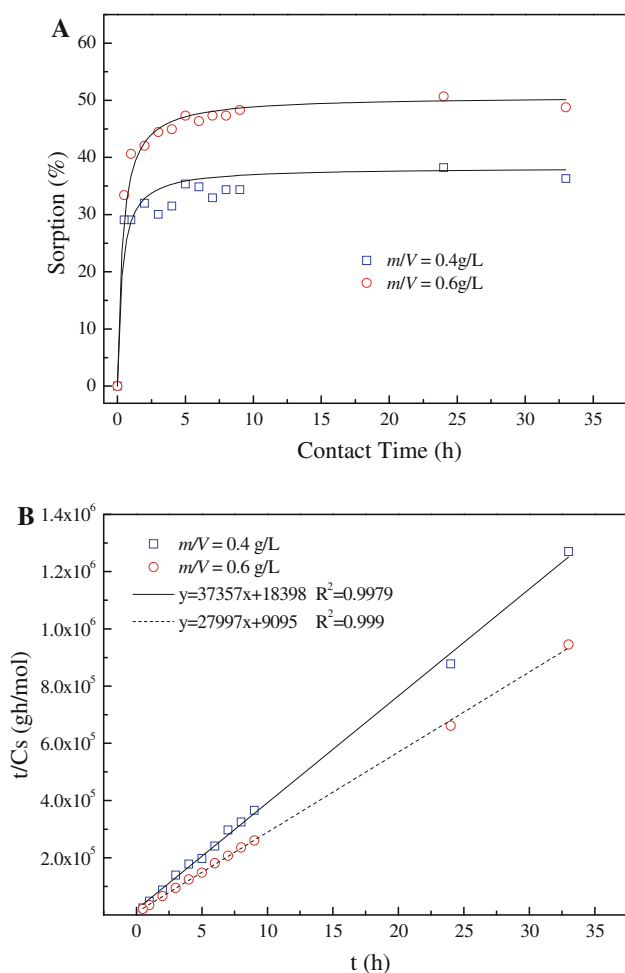
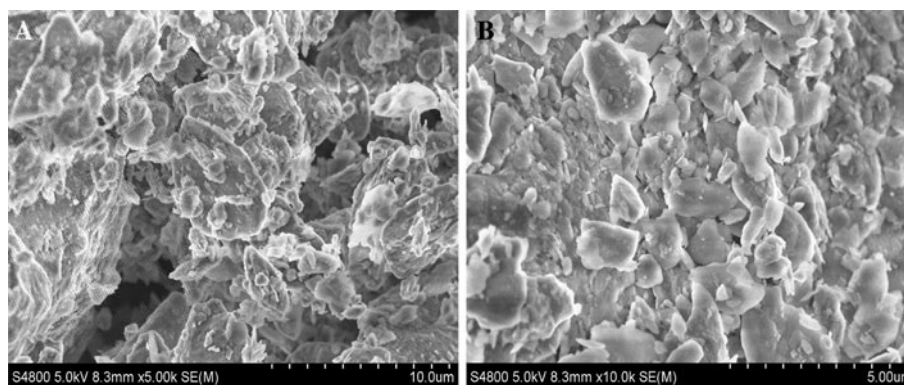


Fig. 3 **a, b** Contact time and the pseudo-second-order of U(VI) sorption onto DCS at m/V 0.4 g/L and 0.6 g/L. $C[\text{UO}_2^{2+}]_{\text{initial}} = 2.86 \times 10^{-5}$ mol/L, $I = 0.05$ mol/L NaClO_4 , pH 6.2 ± 0.1 , $T = 25 \pm 1$ °C

U(VI) adsorbed onto the surface of DCS at time t (h), and C_{max} (mol g^{-1}) is the equilibrium sorption capacity. Linear plots feature of t/C_s vs t were achieved and shown in Fig. 3b. And the correlation coefficient R^2 (equals respective 0.9979 at $m/V = 0.4$ g/L and 0.999 at $m/V = 0.6$ g/L.) of the linear plot are very close to 1, showing the

sorption results can be fitted very well by the pseudo-second-order model. The K' value can be calculated from the slope and intercept of the line, and the values are 7.6×10^4 $\text{g mol}^{-1} \text{h}^{-1}$ for 0.4 g/L and 8.6×10^4 $\text{g mol}^{-1} \text{h}^{-1}$ for 0.6 g/L, respectively.

Effect of solid-to-liquid ratio (m/V)

Effect of m/V on U(VI) sorption to DCS is shown in Fig. 4. Distribution coefficient, K_d (mL/g), can be calculated from the following equation [22]:

$$K_d = \frac{C_0 - C_e}{C_e} \frac{V}{m} 1000 \quad (3)$$

Here, V is the volume of the suspension (L); and m is the mass of the solid (g). It is seen that sorption percent of U(VI) from aqueous phase increases significantly from ~ 20 to $\sim 86\%$ with m/V increasing from 0.1 g/L to 2.0 g/L. As soil content increases in suspension, the number of adsorption sites on the soil surface increases largely and thereby the removal percent of U(VI) increases correspondingly. The distribution coefficient, K_d , values as a function of m/V are also plotted in Fig. 4. Comparing with the strong dependence of U(VI) sorption on solid content, it is seen that K_d is weakly dependent on m/V and increases slightly with the increasing m/V . Similar results were reported by Xu et al. [11]. However, the results of sorption of Sr(II), Eu(III) and U(VI) on compacted bentonite indicated that K_d decreased with increasing bulk density of compacted bentonite [23–26]. Qian et al. [27] found that influence of m/V on sorption of Th(IV) onto $\text{Zr}_2\text{O}(\text{PO}_4)_2$ was also positive, while the K_d value decreased slightly with increasing m/V .

Effect of pH

Sorption of U(VI) on DCS as a function of pH values is shown in Fig. 5. It is clearly seen that U(VI) sorption on DCS is strongly dependent on pH values. The sorption percent of U(VI) increases quickly at pH 4–6, reaches the

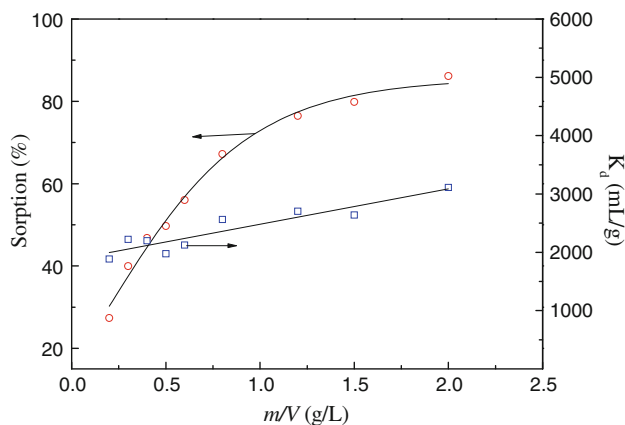


Fig. 4 Effect of m/V on adsorption of U(VI) to DCS. $C[\text{UO}_2^{2+}]_{\text{initial}} = 2.86 \times 10^{-5}$ mol/L, $\text{pH} = 6.2 \pm 0.1$, $T = 25 \pm 1$ °C, $I = 0.05$ mol/L NaClO_4

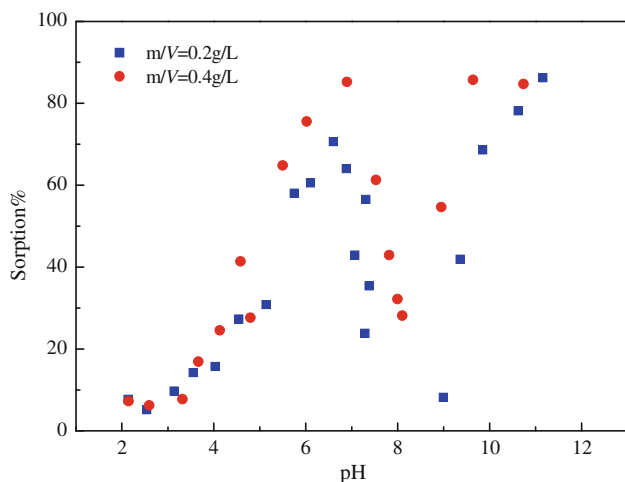


Fig. 5 Effect of pH on U(VI) to DCS. $C[\text{UO}_2^{2+}]_{\text{initial}} = 2.86 \times 10^{-5}$ mol/L, $T = 25 \pm 1$ °C, $I = 0.05$ mol/L NaClO_4

maximum sorption ($\sim 70\%$, $m/V = 0.2$ g/L) at $\text{pH} \sim 7$, and then the removal of uranium goes down between $\text{pH} 7-9$ to $\sim 8\%$ (at $m/V = 0.2$ g/L) and again quickly increases to $\sim 86\%$ when $\text{pH} > 9$. The results at $\text{pH} < 9$ in this work are very similar to those of U(VI) sorption on goethite [1]. Relative speciation of U(VI) as a function of pH values in equilibrium with air ($P_{\text{CO}_2} = 10^{-3.58}$ atm) is shown in Fig. 6. At $\text{pH} < 4$, UO_2^{2+} is the main species ($> 95\%$); at $\text{pH} \sim 7$, the dominant species is $(\text{UO}_2)_2\text{CO}_3(\text{OH})_3^-$ ($\sim 95\%$), the others are only $\sim 5\%$; while $\text{pH} > 9$, the dominant speciation $\text{UO}_2(\text{CO}_3)_3^{4-}$ is $\sim 99\%$, and other species are less than 1%. As we mentioned before, the original calcareous soil was transformed into Ca-type before carbonate was removed, so there would be a certain amount of Ca^{2+} existing in the sorption system. Therefore, it is extrapolated that a complex as $\text{Ca}_2\text{UO}_2(\text{CO}_3)$ was formed in aqueous phase at $\text{pH} > 8$, which is weakly adsorbed to DCS,

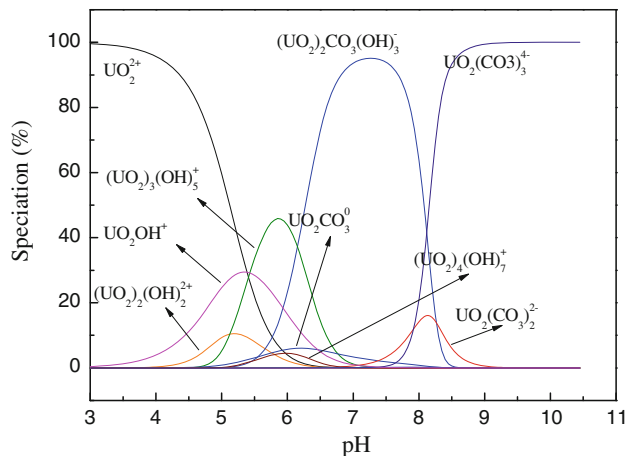


Fig. 6 Uranium speciation in 0.01 mol/L NaClO_4 solution in equilibrium with air ($P_{\text{CO}_2} = 10^{-3.58}$ atm)

resulting in the huge decrease of U(VI) sorption percent at $\text{pH} 7-9$. Zheng et al. [28] also found that the decrease in U(VI) sorption at alkaline pH was related to the increased importance of weakly sorbed aqueous uranium(VI) carbonate complexes $[\text{Ca}_2\text{UO}_2(\text{CO}_3)]$ with increasing pH. At higher pH (> 9), uranium(VI) may precipitate in alkaline solution in the form of $\text{Na}_2\text{U}_2\text{O}_7$, and this sedimentation is separated from aqueous phase through centrifugation.

Effect of temperature

Temperature of the examined system is a very important factor affecting chemicals' reaction properties, thus is treated as a significant parameter in understanding sorption mechanism of radionuclides. Effect of temperature on U(VI) sorption to DCS as a function of pH values is shown in Fig. 7. As can be seen that sorption of U(VI) is

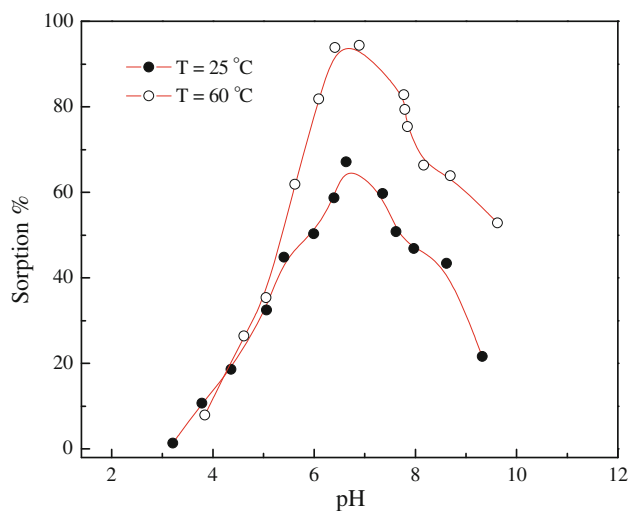


Fig. 7 Influence of temperatures on the U(VI) sorption as a function of pH values. $C[\text{UO}_2^{2+}]_{\text{initial}} = 2.86 \times 10^{-5}$ mol/L, $I = 0.05$ mol/L NaClO_4 , $m/V = 0.4$ g/L

enhanced fairly with the increasing temperature from 25 to 60 °C at neutral pH range. Therefore sorption of U(VI) onto DCS is an endothermic process. Similar results were found in literature that effect of temperature on sorption of heavy metal ions and radionuclides is positive. Fan et al. [29, 30] found that the sorption of Ni(II) to ACT-attapulgite and Th(IV) to attapulgite were both endothermic and negative Gibbs free energy processes. Xie et al. [7] obtained the values of ΔG° all below zero from experimental data of uranium(VI) sorption to hematite at three different temperatures (293, 305, 318 K). However, as Wang et al. [31] has reported, sorption of Eu(III) onto a calcareous soil is adversely influenced by temperature for it decreases with rise in temperature, which indicates an exothermic process.

Sorption isotherms

Figure 8 shows sorption isotherms of uranium to DCS at different m/V . Results show that with increasing m/V sorption of U(VI) is obviously augmented, suggesting that increase in m/V puts a positive influence on uranium sorption. Sorption isotherms are described with the Langmuir and Freundlich models [32]. The Langmuir model assumes that there is no interaction between the adsorbate molecules and the adsorption is localized in a monolayer; the Freundlich model is an empirical relationship describing the adsorption of solutes from a liquid to a solid surface. Equations of the Langmuir and Freundlich sorption models are as follow [1]:

$$\text{Langmuir model: } \frac{C_e}{C_s} = \frac{C_e}{C_{\max}} + \frac{1}{K_L} \quad (4)$$

$$\text{Freundlich model: } \lg C_s = \lg K_F + n \lg C_e \quad (5)$$

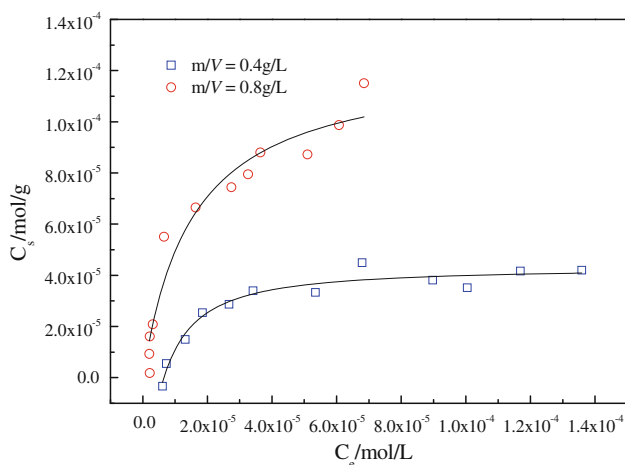


Fig. 8 Effect of m/V on sorption isotherms of U(VI) to DCS. pH 6.2 ± 0.1 , $T = 25 \pm 1$ °C, $I = 0.05$ mol/L NaClO_4

here C_e is the equilibrium concentration of metal ions remained in the solution (mol/L); C_s (mol/g) and C_{\max} (mol/g) are respectively the amount of U(VI) adsorbed to the soil phase and the maximum sorption capacity, and K_L is the sorption reaction equilibrium constant; K_F ($\text{mol}^{1-n} \text{g}^{-1} \text{L}^n$) and n are respectively the sorption capacity when metal ion equilibrium concentration equals to 1 and the degree of dependence of sorption with equilibrium concentration.

Figures 9 and 10 show the sorption patterns of U(VI) at two m/V values fitted with the Langmuir and Freundlich isotherms. Relevant parameters in Langmuir model and Freundlich model are calculated and shown in Table 4. The results indicate that Freundlich model poorly describes the sorption of U(VI) to DCS, and Langmuir model is fitting

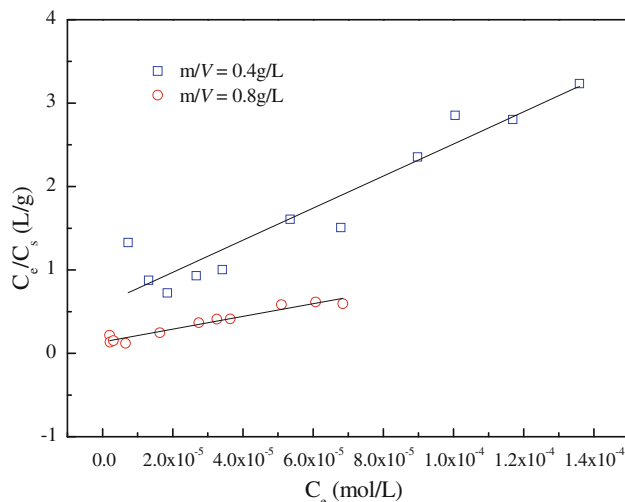


Fig. 9 Langmuir model of U(VI) sorption on DCS

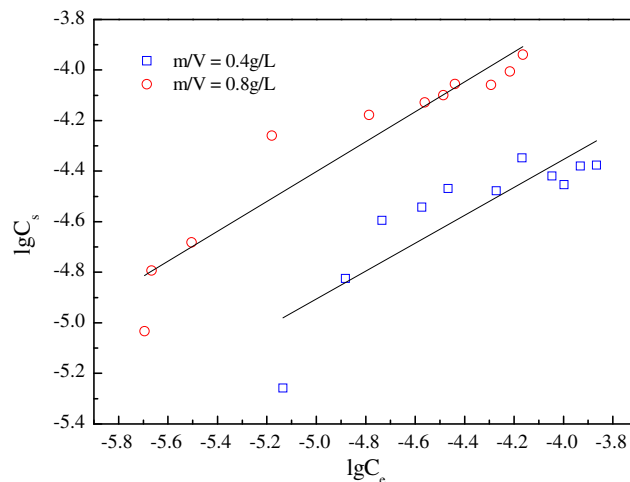


Fig. 10 Freundlich model of U(VI) sorption on DCS

Table 4 Langmuir and Freundlich parameters

| Model | Parameter | $m/V = 0.4$ g/L | $m/V = 0.8$ g/L |
|------------|------------------------------------|-----------------|-----------------|
| Langmuir | C_{\max} (mol/g) | 5.20 E-5 | 1.31 E-4 |
| | K_L | 1.7 | 7.3 |
| | R^2 | 0.8972 | 0.9436 |
| Freundlich | $\lg K_F$ (mol $^{1-n}$ L n /g) | -2.14 | -1.44 |
| | n | 0.55 | 0.59 |
| | R^2 | 0.7257 | 0.8911 |

the sorption of U(VI) to DCS much better than Freundlich model.

Effect of FA on U(VI) sorption

Sorption isotherms of U(VI) in absence and presence of FA is shown in Fig. 11. It is seen that presence of FA could significantly enhance the removal amount of uranium in U(VI) sorption process. At a relatively low concentration (20 mg/L), presence of FA can initially improve U(VI) sorption to DCS drastically. However, as the concentration of FA increases to a much higher degree (50 mg/L, in this work), U(VI) sorption decreases a little comparing with results from low FA concentration system (20 mg/L), which might due to the formation of dissolvable uranyl-humate complexes at high FA concentration. Therefore it is safe to draw the conclusion that the influence of FA on the U(VI) sorption at pH 6.2 is positive, and the lower concentration of FA (20 mg/L) has a better improvement than the higher one (50 mg/L) does on the U(VI) sorption on DCS.

pH sorption edges of U(VI) onto DCS in the presence and absence of FA are shown in Fig. 12. The sorption edge in the presence of FA is shifted to the left about 1 pH unit

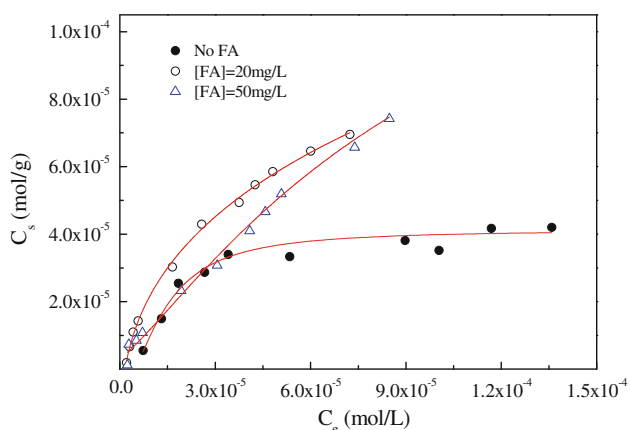


Fig. 11 Effect of FA on sorption isotherm of U(VI) to DCS. $I = 0.05$ mol/L NaClO_4 , pH 6.2 ± 0.1 , $m/V = 0.4$ g/L, $T = 25 \pm 1$ °C

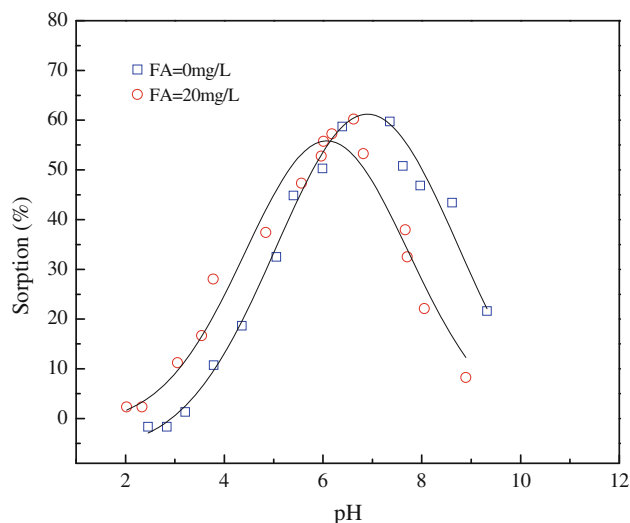


Fig. 12 Effect of FA on U(VI) sorption to DCS as a function of pH values. $C[\text{UO}_2^{2+}]_{\text{initial}} = 2.86 \times 10^{-5}$ mol/L, $I = 0.05$ mol/L NaClO_4 , $m/V = 0.4$ g/L, $T = 25 \pm 1$ °C

comparing with U(VI) sorption in the absence of FA, which indicates a positive influence on U(VI) sorption on DCS at pH < 6.5 and a negative influence at pH > 6.5. However, GUO et al. [33] found that FA of 20 mg/L has little effect on the sorption of U(VI) on goethite, and the sorption of FA is decreased in the presence of U(VI) especially in low pH range. The different influences of FA on U(VI) sorption on materials may be attributed to the different source of FA, or different properties of materials [3]. It is also seen that the influence of presence of FA on U(VI) sorption as shown by results of sorption edges is well consistent with those shown by sorption isotherms.

Effect of FA on sorption–desorption

Effect of FA on the sorption and desorption isotherms is shown in Fig. 13. Figure 13a shows there is a hysteresis in desorption isotherm of U(VI) on DCS comparing to sorption isotherm. It is seen that the concentration of U(VI) on DCS remains stable after the desorption experiments, whereas the concentration of U(VI) in the solution is about one-half of the concentration of U(VI) in the sorption experiment, suggesting that U(VI) sorbed on DCS is scarcely desorbed within testing time, and the sorption of U(VI) on DCS is an irreversible process in the absence of FA. Similarly to conclusions from Li et al. [14], sorption of U(VI) on DCS is ascribed to inner-sphere complex rather than cation exchange/physical sorption. However, in the results of Olguin et al. [34] of UO_2^{2+} sorption onto sodium bentonite (natural bentonite treated with 5 M NaCl solution) 50% of absorbed UO_2^{2+} was observed to desorb after 30 h, which may due to the different sorbent compositions between soil and bentonite causing variant sorption ability.

However, sorption–desorption results in Fig. 13b and c are fairly different in the presence of FA. In Fig. 13b, there is still a slight hysteresis of U(VI) sorption–desorption at higher U(VI) concentrations in 20 mg/L FA solution. However, the sorption and desorption isotherms have no significant difference when the concentration of FA reaches

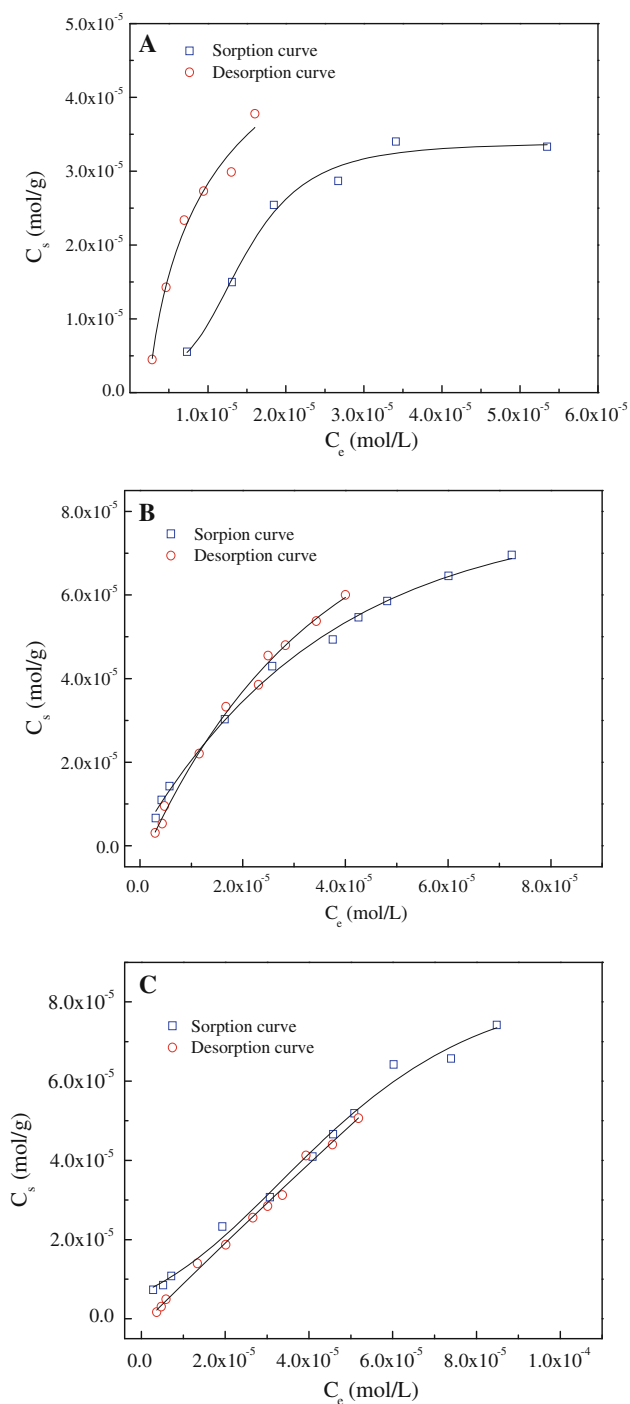


Fig. 13 Effect of the FA existence on U(VI) sorption and desorption isotherms. **a** No FA, **b** [FA] = 20 mg/L, **c** [FA] = 50 mg/L. pH 6.2 ± 0.1 , $T = 25 \pm 1$ °C, $I = 0.05$ mol/L NaClO₄, $m/V = 0.4$ g/L

50 mg/L. This illustrates that the sorption of U(VI) to DCS turns to be a reversible process with the presence of FA. There are two possible reasons for this change, which are: (i) with addition of FA, the combination between soil surface and U(VI) (DCS-U) exchanged for the DCS-FA-U constructure, and the combination between FA and U(VI) is reversible; (ii) FA has a stronger complex ability to uranium than that of DCS, then the U(VI) adsorbed on DCS is dragged into aqueous phase by the free FA molecules in the aqueous solution and form a dissolvable U-humate complexes, resulting in a redistribution of U(VI) in solid–liquid interface.

Effect of CO₂ and carbonates

pH sorption edges of U(VI) on DCS in the presence and absence of CO₂ is shown in Fig. 14. As seen in Fig. 14, the sorption percent of U(VI) is much higher at $P_{CO_2} = 0$ atm than that at $P_{CO_2} = 10^{-3.58}$ atm at about pH > 7. Guo et al. [33] thought the decreasing sorption of U(VI) in high pH range at $P_{CO_2} = 10^{-3.58}$ atm resulted from the complexation of U(VI) and carbonate formed in aqueous phase.

Figure 15 shows FTIR spectra of four samples, which are DCS sample after U(VI) sorption, DCS sample, CaCS sample after adsorbing U(VI) and CaCS sample, respectively. According to FTIR spectra, the broad band from 3620 to 3424 cm⁻¹ is assigned to the stretching vibration of Al–OH groups and HO–H vibration of the water molecules adsorbed on the surface. The peak at 1640 cm⁻¹ corresponds to the bending HO–H bond of water molecules. Peaks at 1024 and 470 cm⁻¹ are attributed to Si–O–Si bonds and the peak at 781 cm⁻¹ may reflect the stretching vibration of Al–O–Si [1, 21]. It is seen that the

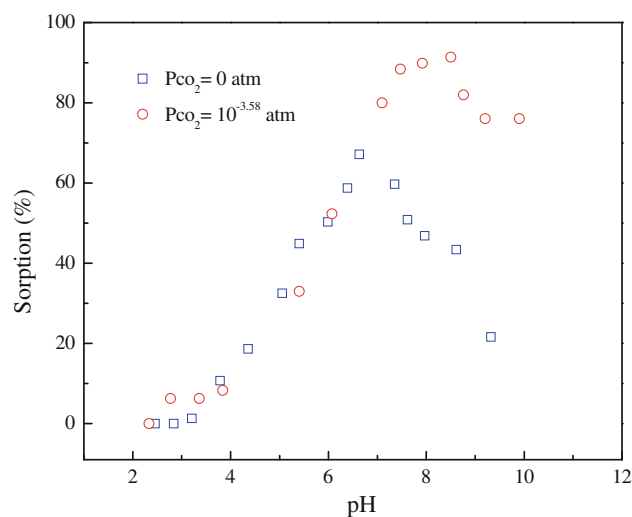


Fig. 14 Effect of CO₂ on U(VI) sorption on DCS as a function of pH values. $C[UO_2^{2+}]_{initial} = 2.86 \times 10^{-5}$ mol/L, $I = 0.05$ mol/L NaClO₄, $m/V = 0.4$ g/L, $T = 25 \pm 1$ °C

peaks at 1434 and 875 cm^{-1} existing in the FTIR spectrum of CaCS sample, referring to the stretching vibration of C–O in carbonates [35], disappear in all samples adsorbed U(VI). This result indicates that carbonate is an important component participating in the sorption reaction between U(VI) and soils. It is also confirmed by the disappeared characterization reflection of carbonate in the spectrum of DCS.

Tests on sorption of U(VI) as a function of pH are carried out both on samples of DCS and CaCS to examine the influence of carbonates in solid phase, and results are shown in Fig. 16. It is easy to notice that sorption of U(VI) is drastically suppressed in high pH range in the sorption to CaCS, while in the low pH range, no obvious difference was observed between two sorption edges. It is estimated that in low pH range, carbonate in CaCS sample is demolished in

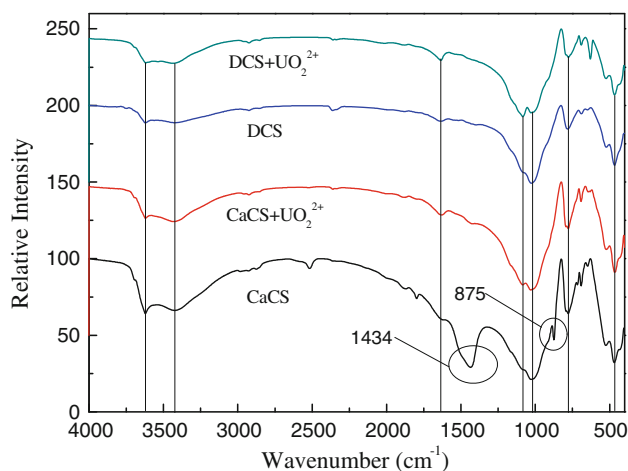


Fig. 15 The FTIR spectra of DCS sample after U(VI) sorption, DCS sample, CaCS sample after U(VI) sorption and CaCS sample

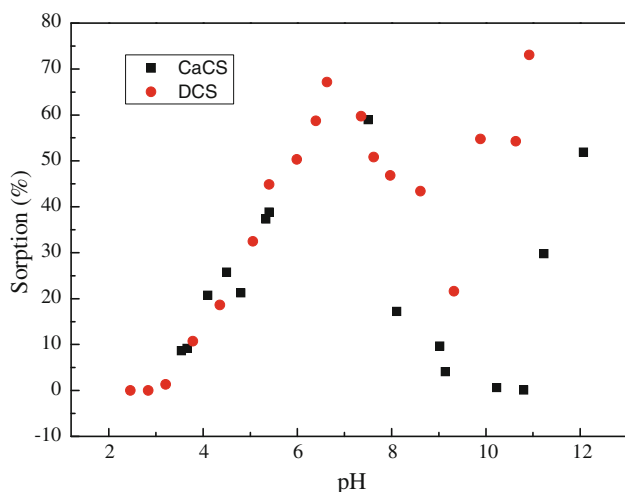


Fig. 16 Effect of pH values on U(VI) sorption on both DCS and CaCS. $C[\text{UO}_2^{2+}]_{\text{initial}} = 2.86 \times 10^{-5} \text{ mol/L}$, $I = 0.05 \text{ mol/L NaClO}_4$, $m/V = 0.4 \text{ g/L}$, $T = 25 \pm 1 \text{ }^\circ\text{C}$

the reaction with the abundant H^+ in aqueous phase, therefore the pH edges of DCS and CaCS are nearly the same because CaCS sample is actually transformed to DCS in the low pH. However, with higher pH values, some sorption of U(VI) to CaCS sample may happen to interaction of uranium with existing carbonate in CaCS sample, so the carbonate structure is changed through sorption process, resulting in the disappearance of peak at 1434 cm^{-1} in FTIR spectrum of CaCS sample after sorption of U(VI).

Conclusions

Based on the results and discussion above, the following main conclusions can be drawn:

- (I) The sorption of U(VI) is strongly dependent on pH values, and there may be a formation of inner-sphere complex at the solid–liquid interface.
- (II) The sorption equilibrium of U(VI) on DCS is very quickly achieved within 5 h, and the results can be well fitted by the pseudo-second-order model.
- (III) U(VI) sorption to DCS increases with increasing of temperature, which suggests the sorption process is endothermic, and Langmuir model is fitting the sorption of U(VI) to DCS much better than Freundlich model;
- (IV) The influence of FA on the U(VI) sorption at pH 6.2 is positive, and the lower concentration of FA (20 mg/L) has a better improvement than the higher one (50 mg/L) does on the U(VI) sorption on DCS. And the presence of FA enhances U(VI) sorption at low pH and reduces the U(VI) sorption at high pH values.
- (V) The sorption of U(VI) on DCS with no FA in the system is irreversible, while the presence of FA transforms U(VI) sorption process a reversible one. And with the presence of CO_2 in the experimental system, there might be a formation of $\text{Ca}_2\text{UO}_2(\text{CO}_3)$ complex in aqueous phase at $\text{pH} > 8$, which is weakly adsorbed to DCS, resulting in a huge decreasing of U(VI) sorption percent in higher pH range.

Acknowledgments Financial support from National Natural Science Foundation of China (No.20871062, J1030932 and J0630962) and National Synchrotron Radiation Innovation Foundation of Chinese Education Ministry (2009) are acknowledged.

References

1. Niu ZW, Fan QH, Wang WH, Xu JZ, Chen L, Wu WS (2009) *Appl Radiat Isot* 67:1582
2. Guo ZJ, Xu J, Shi KL, Tang YQ, Wu WS, Tao ZY (2009) *Colloids Surf A* 339:126

3. Tan XL, Wang XK, Chen CL, Sun AH (2007) *Appl Radiat Isot* 65:375
4. Pathak PN, Choppin GR (2007) *J Radioanal Nucl Chem* 274:53
5. Wu WS, Fan QH, Xu JZ, Niu ZW, Lu SS (2007) *Appl Radiat Isot* 65:1108
6. Guillaumont R, Fanghanel T, Fuger J, Genthe I, Neck V, Palmer A, Rand MH (2003) *Chemical thermodynamics, Volume 5: Update on the chemical thermodynamics of uranium, neptunium, americium and technetium*. Elsevier, Amsterdam, p 970
7. Xie SB, Zhang C, Zhou XH, Yang J, Zhang XJ, Wang JS (2009) *J Environ Radioactiv* 100:162
8. Dong WM, Ball WP, Liu CX, Wang ZM, Stone AT, Bai J, Zachara JM (2009) *Environ Sci Technol* 39:7949
9. Hiemstra T, Riemsdijk WHV, Rossberg A, Ulrich KU (2009) *Geochim Cosmochim Acta* 73:4437
10. Chen CL, Wang XK (2007) *Appl Radiat Isot* 65:155
11. Xu D, Shao DD, Chen CL, Ren AP, Wang XK (2006) *Radiochim Acta* 94:97
12. Montavon G, Markai S, Andres Y, Grambow B (2002) *Environ Sci Technol* 36:3303
13. Xu D, Wang XK, Chen CL, Zhou X, Tan XL (2006) *Radiochim Acta* 94:429
14. Li XL, Chen CL, Chang PP, Yu SM, Wu WS, Wang XK (2009) *Desalination* 244:283
15. Fan QH, Shao DD, Hu J, Chen CL, Wu WS, Wang XK (2009) *Radiochim Acta* 97:141
16. Ticknor KV, Villiks P, Vandergraaf TT (1996) *Appl Geochim* 11:555
17. Wang SW, Hu J, Li JX, Dong YH (2009) *J Hazard Mater* 167(1–3):44
18. Anke M, Seeber O, Müller R, Schäfer U, Zerull J (2009) *Chem Erde-Geochem* 69S2:75
19. <http://ihss.gatech.edu/ihss2/isolation.html>
20. Lu SS, Xu JZ, Zhang CC, Niu ZW. *J Radioanal Nucl Chem*. doi:10.1007/s10967-010-0849-1
21. Chen CL, Wang XK (2006) *Ind Eng Chem Res* 45(26):9144
22. Zhao DL, Feng SJ, Chen CL, Chen SH, Xu D, Wang XK (2008) *Appl Clay Sci* 41:17
23. Wang XK, Liu XP (2004) *Appl Radiat Isot* 61:1413
24. Wang XK, Chen YX, Wu YC (2004) *Appl Radiat Isot* 60:963
25. Wang XK, Rabung Th, Geckeis H, Panak PJ, Klenze R, Fanghaenel Th (2004) *Radiochim Acta* 92:691
26. Wang XK, Liu XP (2005) *Appl Radiat Isot* 62:1
27. Qian LJ, Zhao JN, Hu PZ, Geng YX, Wu WS. *J Radioanal Nucl Chem*. doi:10.1007/s10967-009-0428-5
28. Zheng ZP, Tokunaga TK, Wan JM (2003) *Environ Sci Technol* 37:5603
29. Fan QH, Shao DD, Hu J, Wu WS, Wang XK (2008) *Surf Sci* 602:778
30. Fan QH, Wu WS, Song XP, Xu JZ, Hu J, Niu ZW (2008) *Radiochim Acta* 96:159
31. Wang YQ, Fan QH, Li P, Zheng XB, Xu JZ, Jin YR, Wu WS. *J Radioanal Nucl Chem*. doi:10.1007/s10967-010-0809-9
32. Li Y, Di Z, Ding J, Wu D, Luan Z, Zhu Y (2005) *Water Res* 39:605
33. Guo ZJ, Li Y, Wu WS (2009) *Appl Radiat Isot* 67:996
34. Olguin MT, Solache-Rios M, Acosta D, Bosch P, Bulbulian S (1997) *J Radioanal Nucl Chem* 218:65
35. Bosch Reig F, Gimeno Adelantado JV, Moya Moreno MCM (2002) *Talanta* 58:811